Electronic Supplementary Material (ESI) for Physical Chemistry Chemical Physics.

Highly selective uptake of carbon dioxide on the zeolite $|Na_{10.2}KCs_{0.8}|$-LTA – a possible sorbent for biogas upgrading

Ocean Cheung[a,b], Dariusz Wardecki[a], Zoltán Bacsik[a], Petr Vasiliev[c], Lynne B. McCusker[a,d] and Niklas Hedin[a]

a. Department of Materials and Environmental Chemistry and Berzelii Center EXSELENT on Porous Materials, Stockholm University, SE-106 91 Stockholm, Sweden. E-mail: niklas.hedin@mmk.su.se

b. Nanotechnology and Functional Materials, Department of Engineering Sciences, Uppsala University, SE-751 21 Uppsala, Sweden

c. NeoZeo AB, Villa Bellona, Universitetsvägen 10A, SE-106 91 Stockholm, Sweden.

d. Laboratory of Crystallography, ETH Zürich, Wolfgang-Pauli-Strasse 10, CH-8093 Zürich,

Supporting information

Experimental procedures

Preparation of the zeolites |Na-K|-LTA, |Na-Cs|-LTA and |Na-K-Cs|-LTA

Highly crystalline zeolite A ($|Na_{12}|$-**LTA**) powder was obtained from Shanghai Cinmore Import & Export Co., Ltd, China. The Na^+, K^+ and Cs^+ forms of zeolite A used in this study were obtained using a one- or two-step partial-ion-exchange process. The procedures for partial K^+ ion exchange can be found in Liu et al.[21] The equivalent procedures can be adopted for partial Cs^+ ion exchange. Here, the steps for preparing $|Na_{10.2}KCs_{0.8}|$-**LTA** with approximately 8 atomic% K^+, 7 atomic% Cs^+ and 85 atomic% Na^+ is given as an example. 2

g of |Na_{12}|-**LTA** was mixed in 100 mL of a 0.01 M solution of KCl for 30 minutes at room temperature to produce |$Na_{11}K$|-**LTA**, which was then separated from the solution, washed and dried at 373K for 2 hours. This zeolite (2 g) was then mixed in 100 mL of a 0.01 M solution of CsCl for 30 minutes at room temperature. The final product was the zeolite |$Na_{10.2}KCs_{0.8}$|-**LTA**, which was again separated from the solution, washed and dried at 373K for 2 hours.

The ion-exchanged zeolites |$Na_{11}K$|-**LTA** and |$Na_{11}Cs$|-**LTA** can be produced via a single step ion-exchange process, similar to that discussed above but without a second step.

The cation compositions of the ion-exchanged zeolites were determined using energy dispersive X-ray spectroscopy (EDX) and then further confirmed with inductive coupled plasma – optical emission spectroscopy (ICP-OES) by Medac Ltd, UK. EDX analysis was performed on a Hitachi TM3000 electron microscope in "analysis" mode with an accelerating voltage of 15kV. For the latter, the samples were spread onto a carbon film on an aluminium support and placed in a vacuum chamber.

Gas adsorption measurements

Gas adsorption (CO_2 and CH_4) isotherms of the zeolite samples were recorded on a Micromertrics ASAP2020 surface area analyser at 293K. The temperature of the analyses was controlled by a Julabo CF31 temperature control unit. A low molecular weight siloxane polymer was used as the heat transfer medium. Equilibrium uptake of the sample was calculated when the change in pressure of the analysis setup fell below 0.01% for 20 s intervals (with a minimum 200 s delay). Before the analyses, all samples were pre-treated/degassed by heating to 623K under high dynamic vacuum (1×10^{-4} Pa) for 6 hours. This degassing step removes the occluded water molecules from the zeolite.

Cyclic CO_2 adsorption measurements of $|Na_{10.2}KCs_{0.8}|$**-LTA** were performed at 293K using a Micromertrics Gemini V 2390 surface area analyser with a room temperature add on. The temperature of the analyses was controlled by a Huber Ministat 230 temperature control unit. A low molecular weight siloxane polymer was used as the heat transfer medium. Equilibrium uptake of the sample was calculated when the change in pressure of the analysis setup fell below 0.01% for 10 s intervals (with a minimum 100 s delay). All samples were pre-treated/degassed at 623K under a slow flow of dry N_2 gas for 6 hours before the first cycle. In between subsequent cycles, the sample was regenerated simply by treating it with dynamic vacuum (0.07 kPa) for 60 minutes at room temperature. The majority of the chemisorbed CO_2 and possibly some trapped physisorbed CO_2 were not removed in this process.

In this study, the CO_2/CH_4 selectivity is defined in terms of the “separation factor” first proposed by Mair.[23] The selectivity (s) was calculated using $s = (q_{CO2}/q_{CH4})/(p_{CO2}/p_{CH4})$, where p_x represents the partial pressure of component x in the mixed gas stream, q_x is the amount of uptake of component x at pressure p_x using the data from pure gas adsorption isotherms. For the purpose of data analysis, the gas is assumed to be a 50:50 volume mixture of CO_2 and CH_4, the pressure of the gas stream is 1 bar.

Diffraction Studies

The crystal structures of dehydrated $|Na_{10.2}KCs_{0.8}|$**-LTA**, $|Na_{10.6}K_{0.8}Cs_{0.6}|$**-LTA**, and $|Na_{10.6}K_{0.6}Cs_{0.8}|$**-LTA** were studied using high-resolution powder diffraction data collected on beamline ID-22 at the ESRF with a wavelength of 0.4009(1) Å. Prior to the diffraction study, the samples were filled into borosilicate glass capillaries (∅ = 0.7 mm), pretreated at 623 K in the oven, mounted in the gas cell and again heated at 523K under dynamic vacuum for 1 hour. The diffraction patterns were measured at room temperature (Table S1). The data were analysed using the Rietveld method coupled with difference Fourier analysis using the program Topas [A.A. Cohelo, Topas-Academic v4.1: www.topas-academic.net]. The refined parameters are listed in Tables S2-5 and calculated profile fits are shown in Figure S1. Examination of the difference Fourier map after the initial Na^+, K^+ and Cs^+ ion positions had been added to the model revealed an additional Cs^+ position at Cs(2). The occupancy of this position is relatively low but it changes with Cs content. The total number of Cs^+ ions in the 8-ring calculated from the refinement is 0.88(3) for $|Na_{10.2}KCs_{0.8}|$-**LTA**, 0.56(2) for $|Na_{10.6}K_{0.8}Cs_{0.6}|$-**LTA**, and 0.88(3) for $|Na_{10.6}K_{0.6}Cs_{0.8}|$-**LTA**. Although there are small discrepancies between the calculated values and the reference values, they are within reason and show an appropriate trend. The same trend is seen for the numbers of Na^+ and K^+ ions in the 8-rings. The refined occupancies for the positions Na(2) and K(1) are 1.0(1) and 1.4(1) atoms per unit cell in $|Na_{10.2}KCs_{0.8}|$-**LTA**, 1.7(1) and 1.3(1) in $|Na_{10.6}K_{0.8}Cs_{0.6}|$-**LTA**, 1.6(1) and 1.1(1) in $|Na_{10.6}K_{0.6}Cs_{0.8}|$-**LTA**, respectively. The total number of cations for each sample is 11.9(2) in $|Na_{10.2}KCs_{0.8}|$-**LTA**, 12.2(2) in $|Na_{10.2}KCs_{0.8}|$-**LTA**, and 12.2(2) in $|Na_{10.6}K_{0.8}Cs_{0.6}|$-**LTA**. The discrepancies might be due to the presence of a small amount of water in the structure. The difference electron density maps revealed two peaks, one in the α-cage and the other in the β-cage. These could be assigned as water positions and were included in the final model. However, there may be additional (disordered) water positions that were not located and therefore not refined.

To test the influence of residual water, we performed an additional test with zeolite $|Na_{12}|$-**LTA** that shows that the dehydration level of the sample has a direct influence on the occupancies of the cations in the 8-ring. During the test, we collected a series of X-ray powder diffraction patterns using a PANalytical X'pert PRO laboratory diffractometer (CuKα radiation) with the sample in a vacuum chamber (~10^{-2} mbar). Figure S2 shows how the occupancies of the cations in the three rings change during the annealing process. One can see that for the position in the 8-ring, the occupancy only reaches the ideal value of 3 per unit cell above 300°C.

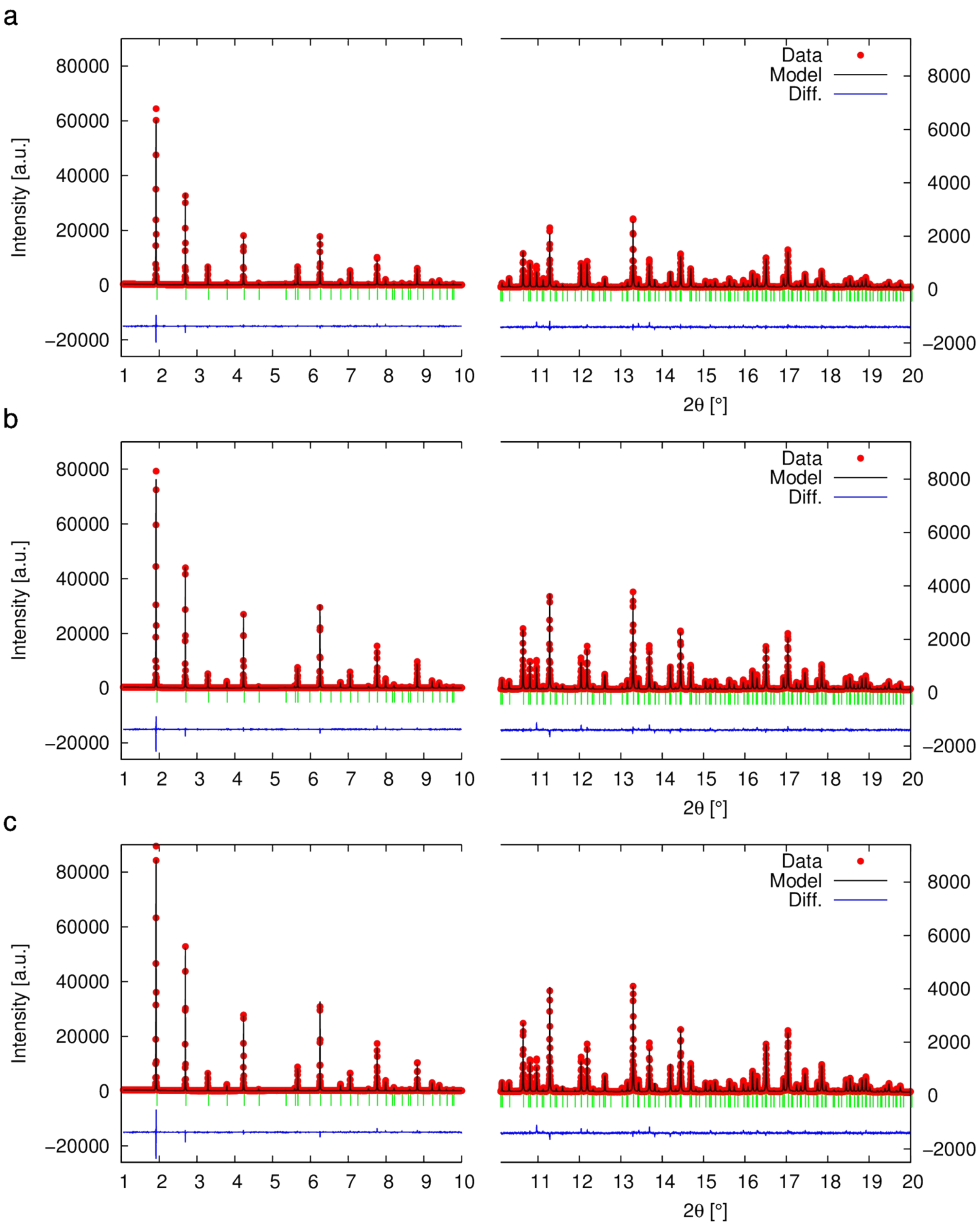

Figure S1. Observed (red), calculated (black) and difference (blue) profiles for the Rietveld refinement of (a) $|Na_{10.6}K_{0.8}Cs_{0.6}|$-**LTA**, (b) $|Na_{10.6}K_{0.6}Cs_{0.8}|$-**LTA**, (c) $|Na_{10.2}KCs_{0.8}|$-**LTA**.

The scale has been increased by a factor of approximately 10 for the high angle range to show more detail.

Table S1. Crystallographic data for the three dehydrated zeolites.

Sample	$\|Na_{10.6}K_{0.8}Cs_{0.6}\|$-**LTA**	$\|Na_{10.6}K_{0.6}Cs_{0.8}\|$-**LTA**	$\|Na_{10.2}KCs_{0.8}\|$-**LTA**
Beamline	ESRF ID-22	ESRF ID-22	ESRF ID-22
Wavelength (Å)	0.4009(1)	0.4009(1)	0.4009(1)
2θ range (°)	1.00 - 30.00	1.00 - 30.00	1.00 - 30.00
Step size (°)	0.002	0.002	0.002
Space group	$Fm\overline{3}c$	$Fm\overline{3}c$	$Fm\overline{3}c$
a (Å)	24.5803(1)	24.5813(1)	24.5778(1)
Reflections	472	472	472
Parameters	60	60	60
Restraints	6	6	6
R_I	0.027	0.030	0.032
R_{wp}	0.069	0.061	0.066
R_{exp}	0.025	0.020	0.028
GOF	2.8	3.0	2.3

Table S2. Atomic positions, occupancies and displacements for $|Na_{10.2}KCs_{0.8}(H_2O)_{3.9}|$ $[Al_{12}Si_{12}O_{48}]$-**LTA**.

Atom	**Site**	***x***	***y***	***z***	**occ.**	B_{iso}
Si	96*i*	0	0.0924(1)	0.1842(1)	1	0.8(1)
Al	96*i*	0	0.1872(1)	0.0902(1)	1	1.3(1)
O(1)	96*i*	0	0.1125(1)	0.2462(1)	1	1.8(1)
O(2)	96*i*	0	0.1471(2)	0.1484(2)	1	1.5(1)
O(3)	192*j*	0.0530(1)	0.0577(1)	0.1688(1)	1	2.0(1)
Na(1)	64*g*	0.1016(1)	0.1016(1)	0.1016(1)	0.944(4)	3.7(1)[a]
Na(2)	96*i*	0	0.228(2)	0.206(2)	0.08(1)	3[b]
Na(3)	96*h*	¼	0.1405(5)	0.1405(5)	0.085(2)	3[b]

Cs(1)	96*i*	0	¼	¼	0.211(4)	3^b
Cs(2)	96*i*	0.028(1)	¼	¼	0.040(2)	3^b
K(1)	96*i*	0	0.2181(1)	0.236(2)	0.12(1)	3^b
Ow(4)	64*g*	0.3227(3)	0.3227(3)	0.3227(3)	0.225(3)	3^b
Ow(5)	48*e*	0.0727(3)	0	0	0.353(2)	3^b

^{a} isotropic equivalent of ADP's $U_{11}=U_{22}=U_{33}=0.051(1)$ and $U_{12}=U_{13}=U_{23}=0.044(1)$
^{b} value fixed

Table S3. Selected interatomic distances (Å) and angles (°) for $|Na_{10.2}KCs_{0.8}(H_2O)_{3.9}|$**$[Al_{12}Si_{12}O_{48}]$-LTA**.

Si – O(1)	1.60(1)	O(1) – Si – O(2)	105.1(1)
Al – O(1)	1.73(1)	O(1) – Si – O(3)	112.8(1)
Na(1) – O(2)	2.97(1)	O(2) – Si – O(3)	108.8(1)
Na(1) – O(3)	2.31(1)	O(1) – Al – O(2)	106.0(1)
Na(2) – O(1)	2.39(1)	O(1) – Al – O(3)	114.2(1)
Na(2) – O(2)	2.45(1)	O(2) – Al – O(3)	106.7(1)
Na(3) – O(1)	3.52(1)		
Na(3) – O(3)	3.57(1)		
K(1) – O(1)	2.61(1)		
K(1) – O(2)	2.78(1)		
Cs(1) – O(1)	3.38(1)		
Cs(1) – O(2)	3.55(1)		

Table S4. Atomic positions, occupancy and displacements for $|Na_{10.6}K_{0.8}Cs_{0.6}\,(H_2O)_{4.0}|[Al_{12}Si_{12}O_{48}]$**-LTA**.

Atom	**Site**	***x***	***y***	***z***	**occ.**	B_{iso}
Si	96*i*	0	0.0925(1)	0.1841(1)	1	1.0(1)
Al	96*i*	0	0.1876(1)	0.0898(1)	1	1.2(1)
O(1)	96*i*	0	0.1128(1)	0.2462(1)	1	2.3(1)
O(2)	96*i*	0	0.1473(2)	0.1484(2)	1	1.3(1)
O(3)	192*j*	0.0527(1)	0.0578(1)	0.1693(1)	1	2.3(1)
Na(1)	64*g*	0.1022(1)	0. 1022(1)	0. 1022(1)	0.975(4)	4.5(1)[a]
Na(2)	96*i*	0	0.237(2)	0.200(1)	0.14(1)	3[b]
Na(3)	96*h*	¼	0.1382(5)	0.1382(5)	0.095(2)	3[b]
Cs(1)	96*i*	0	¼	¼	0.126(4)	3[b]
Cs(2)	96*i*	0.039(1)	¼	¼	0.030(1)	3[b]
K(1)	96*i*	0	0.217(1)	0.226(1)	0.11(4)	3[b]
Ow(4)	64*g*	0.3221(3)	0.3221(3)	0.3221(3)	0.251(4)	3[b]
Ow(5)	48*e*	0.0735(3)	0	0	0.330(3)	3[b]

[a] isotropic equivalent of ADP's $U_{11}= U_{22}= U_{33}$=0.060(1) and $U_{12}= U_{13}= U_{23}$=0.054(1)
[b] value fixed

Table S5: Atomic positions, occupancy and displacements for $|Na_{10.6}K_{0.6}Cs_{0.8}\,(H_2O)_{3.8}|[Al_{12}Si_{12}O_{48}]$**-LTA**.

Atom	**Site**	***x***	***y***	***z***	**occ.**	B_{iso}
Si	96*i*	0	0.0925(1)	0.1841(1)	1	0.86(4)
Al	96*i*	0	0.1873(1)	0.0902(1)	1	1.26(5)
O(1)	96*i*	0	0.1112(1)	0.2462(1)	1	1.7(1)
O(2)	96*i*	0	0.1470(2)	0.1484(2)	1	1.5(1)
O(3)	192*j*	0.0531(1)	0.0578(1)	0.1688(1)	1	1.89(4)
Na(1)	64*g*	0.1015(1)	0. 1015(1)	0. 1015(1)	0.933(4)	3.0(1)[a]
Na(2)	96*i*	0	0.227(1)	0.210(1)	0.13(1)	3[b]
Na(3)	96*h*	¼	0.1426(5)	0.1426(5)	0.071(2)	3[b]
Cs(1)	96*i*	0	¼	¼	0.213(5)	3[b]
Cs(2)	96*i*	0.028(1)	¼	¼	0.040(1)	3[b]

K(1)	96*i*	0	0.222(1)	0.240(2)	0.09(1)	3[b]
Ow(4)	64*g*	0.3212(3)	0.3212(3)	0.3212(3)	0.201(3)	3[b]
Ow(5)	48*e*	0.0738(3)	0	0	0.368(2)	3[b]

[a] isotropic equivalent of ADP's $U_{11}= U_{22}= U_{33}=0.042(1)$ and $U_{12}= U_{13}= U_{23}=0.035(1)$
[b] value fixed

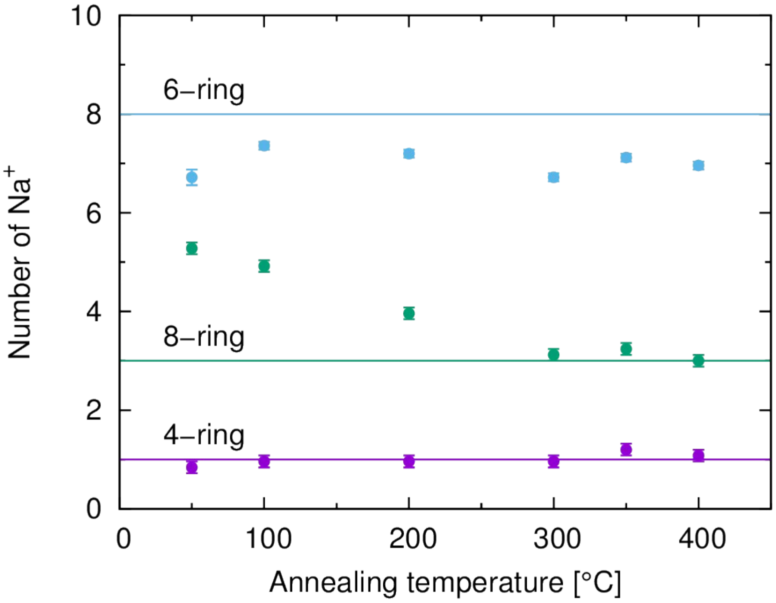

Figure S2. The number of Na$^+$ cations in |Na$_{12}$|-**LTA** as a function of thermal treatment under vacuum. Refined occupancies of the three Na$^+$ sites (6-ring: blue, 8-ring: green and 4-ring: purple) are shown as circles and the ideal values as lines.

In situ infrared spectroscopy

The infrared (IR) spectra were recorded on a Varian 670-IR FT-IR spectrometer using a mercury cadmium telluride (MCT) detector cooled with liquid nitrogen. The *in situ* experiments were performed with a high vacuum stainless steel manifold connected to a stainless steel IR transmission cell. Samples of |Na$_{10.2}$KCs$_{0.8}$|-**LTA** (~ 25 mg) were pressed into pellets with a pressure of 1 x 10^9 kg/m^2 for 2 minutes. The pellets were heated to 523K under high dynamic vacuum (<1 x10^{-4} Pa) in the IR cell for a minimum of 6 hours before the *in situ* measurement. After degassing, CO_2 was let into the IR cell and the spectra were recorded as a function of the CO_2 pressure and time. A detailed description of this experiment has been published previously. [22, 24]

The physisorption rate was measured by *in situ* IR spectroscopy by following the development of a combination band of adsorbed CO_2. During this experiment, the pre-treated sample was subjected to 13.3 kPa of CO_2. The development of a band (3598 cm^{-1}) was monitored with respect to exposure time. The intensity of the band was normalised against the equilibrium intensity (recorded when there were no noticeable changes in the intensity of the band).

Results and discussion

Additional adsorption isotherms

Cs$^+$ ion-exchanged zeolite A (|Na-Cs|-**LTA**) as CO_2 adsorbent

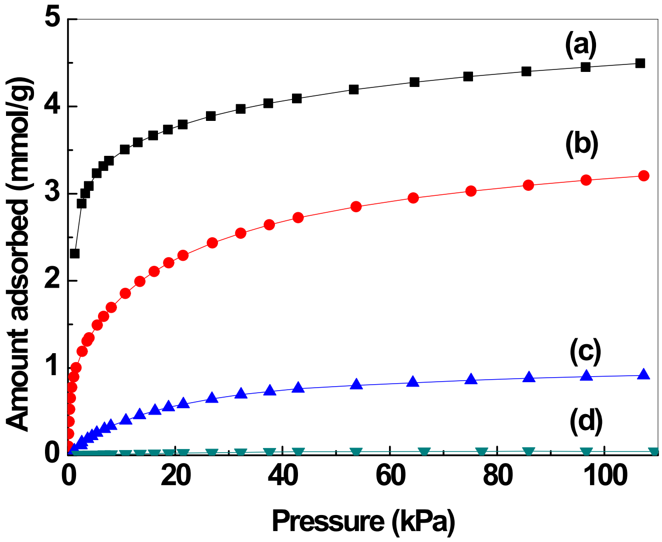

Figure S3. CO_2 adsorption isotherms for |Na-Cs|-**LTA** with different amounts of Cs$^+$. (a) (|$Na_{12}Cs_0$|-**LTA**), (b) (|$Na_{11}Cs_1$|-**LTA**), (c) (|$Na_{10}Cs_2$|-**LTA**) and (d) (|$Na_{8.6}Cs_{3.4}$|-**LTA**).

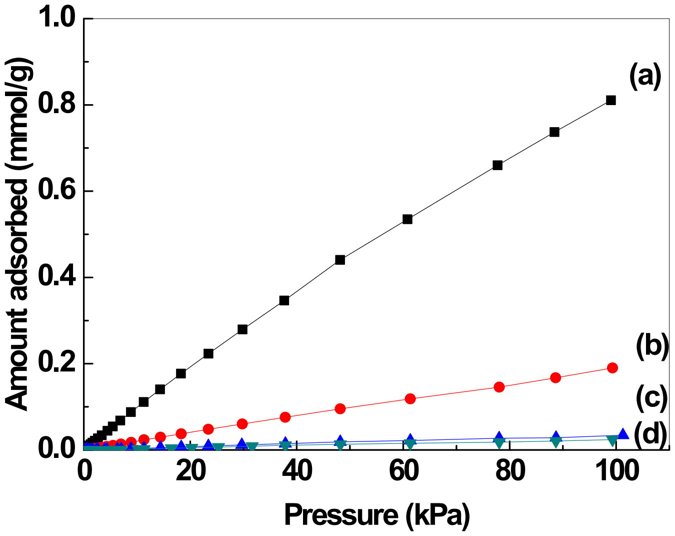

Figure S4. CH_4 adsorption isotherms for |Na-Cs|-**LTA** with different amounts of Cs^+. (a) (|$Na_{12}Cs_0$|-**LTA**), (b) (|$Na_{11}Cs_1$|-**LTA**), (c) (|$Na_{10}Cs_2$|-**LTA**) and (d) (|$Na_{8.6}Cs_{3.4}$|-**LTA**). Both (c) and (d) show very little CH_4 uptake.

K^+ ion-exchanged zeolite A (|Na-K|-**LTA**) as CO_2 adsorbent

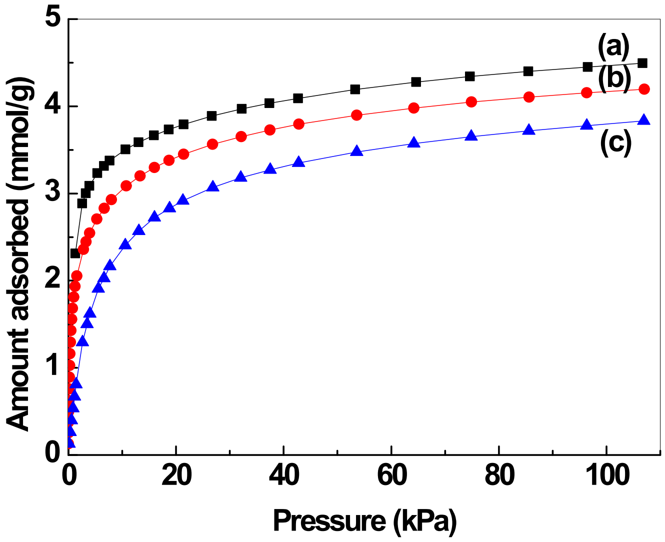

Figure S5. CO_2 adsorption isotherms for |Na-K|-**LTA** with different amounts of K^+.

(a) (|$Na_{12}K_0$|-**LTA**), (b) (|$Na_{11}K_1$|-**LTA**) and (c) (|$Na_{10}K_2$|-**LTA**).

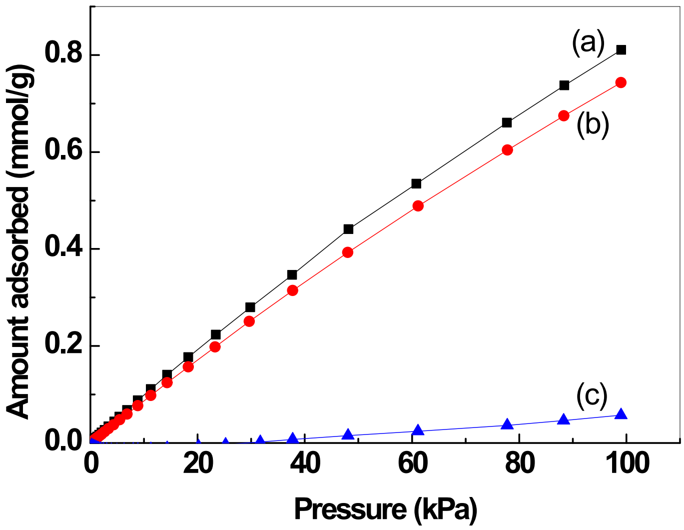

Figure S6. CH_4 adsorption isotherms for |Na-K|-**LTA** with different amounts of K^+. (a) ($|Na_{12}K_0|$-**LTA**), (b) ($|Na_{11}K_1|$-**LTA**) and (c) ($|Na_{10}K_2|$-**LTA**).

CO_2 physisorption kinetics

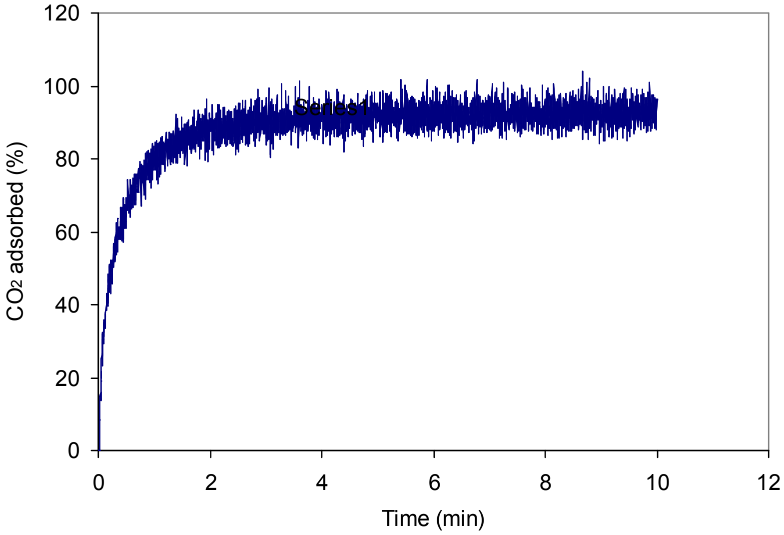

Figure S7. CO_2 physisorption kinetics for $|Na_{10.2}KCs_{0.8}|$-**LTA** data recorded at 13.3 kPa and 303K .

IR spectroscopy

Additional information

Chemisorption of CO_2 could be characterised with IR bands in the region of 1400 to 1750 cm^{-1}. The presence of three different types of cations resulted in a mixture of different types of chemisorbed CO_2. Their respective IR bands are difficult to assign because they occur at similar frequencies, but they are consistent with a variety of carbonate and carbonate-like species.

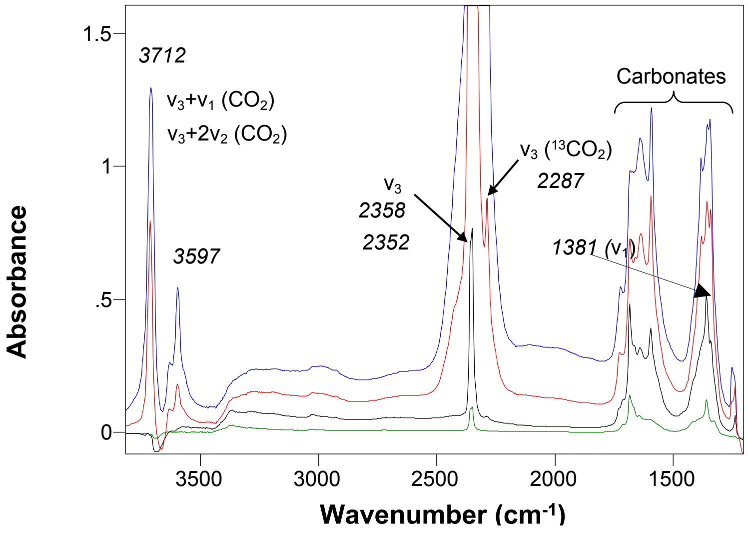

Figure S8. IR spectra of CO_2 adsorbed on **$|Na_{10.2}KCs_{0.8}|$-LTA**, adsorption branch at CO_2 pressures of 0.013 kPa, 0.040 kPa, 1.3 kPa and 13.3 kPa (bottom to top) Even at low CO_2 pressures, the band for the symmetric stretching υ_1, which is normally IR inactive, appeared at 1381 cm^{-1} as a result of the distortion of the symmetry of the physisorbed CO_2.

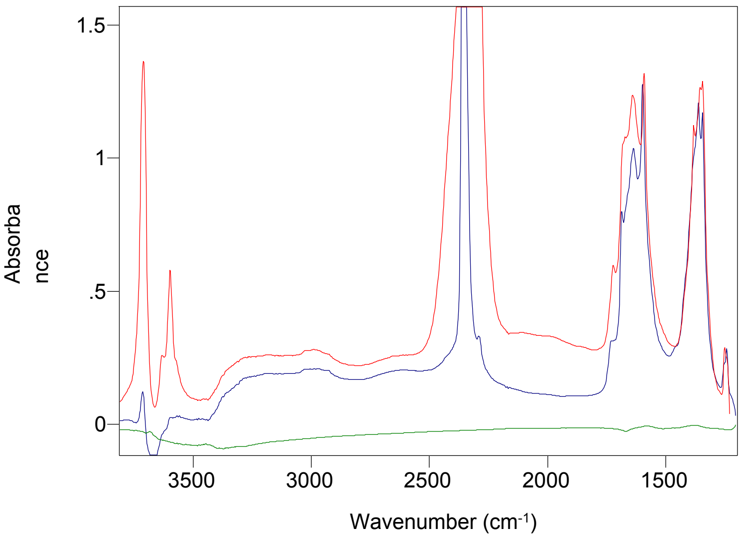

Figure S9. IR spectra of CO_2 adsorbed on |$Na_{10.2}KCs_{0.8}$|-**LTA** in the desorption branch, at a CO_2 pressure of 13.3 kPa (green), after 20 minutes evacuation (blue) and after heat regeneration (red).